Supporting Information for "Paleointensity Estimates from the Pleistocene of Northern Israel: Implications for hemispheric asymmetry in the time averaged field"

L.Tauxe[1], H. Asefaw[1], N. Behar[2], A.A.P. Koppers[3], R. Shaar[2]

[1]Geosciences Research Division, Scripps Institution of Oceanography, University of California San Diego, La Jolla, CA, USA

[2]The Institute of Earth Sciences, Hebrew University of Jerusalem, Jerusalem, Israel

[3]College of Earth, Ocean, and Atmospheric Sciences, Oregon State University, Corvallis, OR, USA

Contents of this file

1. Figure S1
2. Table S1 to S10

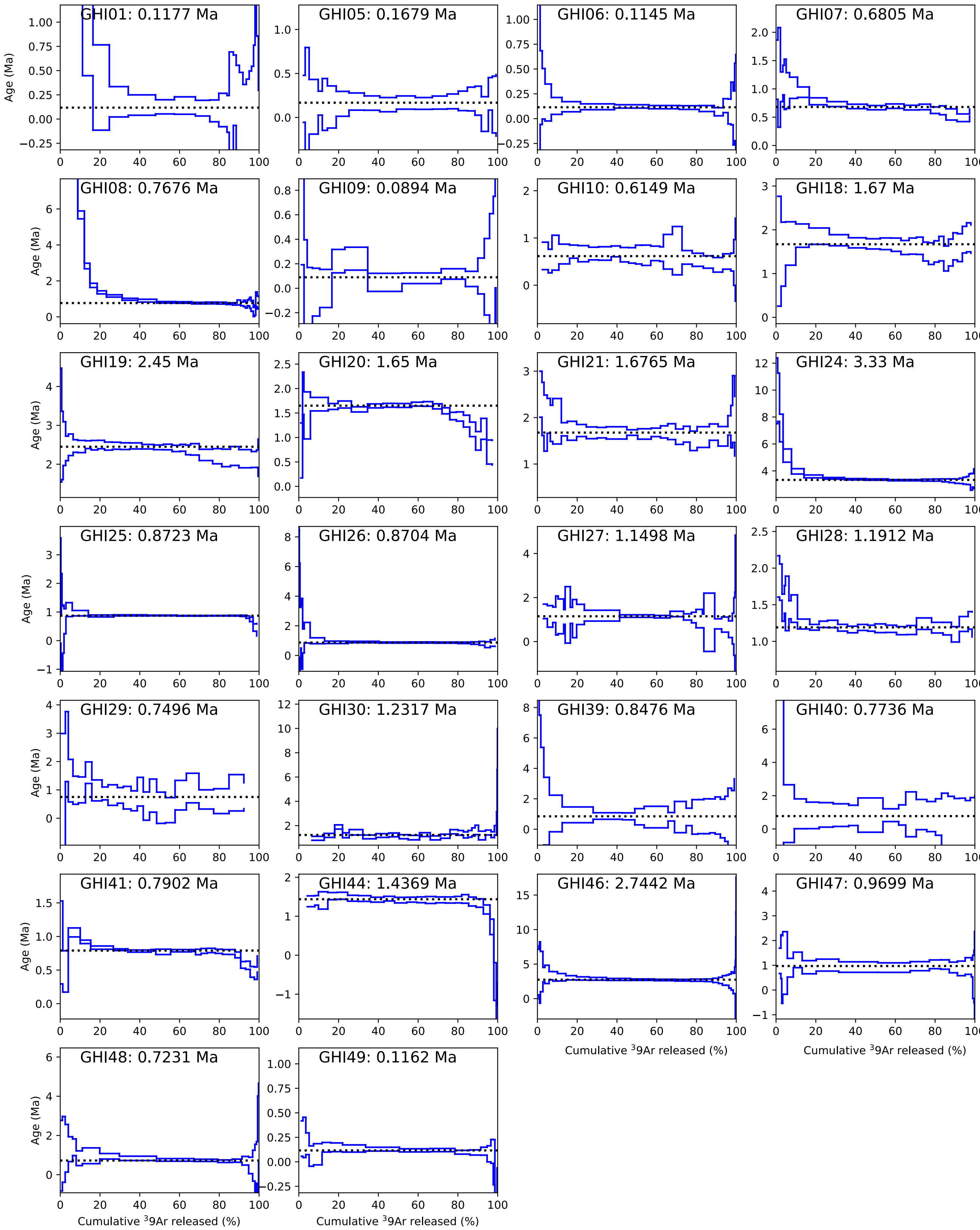

Figure S1. $^{40}Ar/^{39}Ar$ age spectra of 26 sites dated in this study. Site ages were determined based on the plateau age or in two cases a mini-plateau (GHI30 and GHI44), see Table c.)

Site	Location name	Age (ka)	$\pm 2\sigma$ (ka)	Latitude	Longitude	Age Reference
GHI01	Mt. Bental	117.7	35.80	33.126350	35.782270	This Study
GHI02*	Mt. Bar-On	129.6	12	33.158050	35.776730	Weinstein et al. (2020)
GHI03	Tel Sheivan	842.0	23.3	33.122790	35.724160	Weinstein et al. (2020)
GHI04	Gamla			32.910040	35.763120	
GHI05	Tel Peres	167.9	25.5	32.960510	35.862240	This Study
GHI06	Mt. Shifon	114.5	8.5	33.069580	35.771430	This Study
GHI07	Ortal	680.5	18.3	33.085810	35.755890	This Study
GHI08	Mt. Hermonit	767.6	17.9	33.178820	35.792360	This Study
GHI09	Mt. Odem	89.4	25.1	33.194300	35.752930	This Study
GHI10	Bashanit	614.9	34.95	33.051680	35.849680	This Study
GHI11	Revaia Quarry			32.449722	35.463838	
GHI12	Alumot Junction			32.717222	35.550282	
GHI13	Karnei Hittin quarry			32.805278	35.457625	
GHI14	Karnei Hittin quarry			32.805556	35.458190	
GHI15	Karnei Hittin quarry			32.805556	35.458190	
GHI16	Mt. Dalton			33.025556	35.496324	
GHI17	Mt. Dalton			33.025556	35.496324	
GHI18	Mt. Dalton	1670	40	33.025833	35.494912	
GHI19	Amuka	2450.0	22.6	32.995278	35.525986	This Study
GHI20	Givat Orcha	1650	20	32.926290	35.849940	
GHI21	Givat Orcha	1676.5	30.2	32.926290	35.849940	This Study
GHI22	Givat Orcha			32.926290	35.849940	
GHI23	Mt. Ram			33.249190	35.789400	
GHI24	Mt. Ram	3330.0	20.00	33.248483	35.790110	This Study
GHI25	Mt. Ram	872.3	5.3	33.218726	35.777062	This Study
GHI26	Mt. Kramin	870.4	16.9	33.220000	35.776833	This Study
GHI27	Mt. Varda	1149.8	34.8	33.212500	35.786157	This Study
GHI28	Mt. Varda	1191.2	15.2	33.212500	35.786157	This Study
GHI29	Mt. Hermonit	749.6	94.50	33.179444	35.793218	This Study
GHI30	Mt. Hermonit	1231.7	75.7	33.182056	35.798538	This Study
GHI31	Nahal Orvim			33.141000	35.679000	
GHI32	Nahal Orvim			33.141000	35.680000	
GHI33	Nahal Orvim			33.141000	35.680000	
GHI34	Nahal Orvim			33.141000	35.680000	
GHI35	Nahal Orvim			33.141000	35.680000	
GHI36	Nahal Orvim			33.141000	35.680000	
GHI37	Nahal Orvim			33.142000	35.679000	
GHI38	Nahal Orvim			33.142000	35.679000	
GHI39	Nahal Orvim	847.6	116.50	33.141000	35.682000	This Study
GHI40	Nahal Orvim	773.6	194.90	33.141000	35.682000	This Study
GHI41	Nahal Orvim	790.2	5.80	33.141000	35.683000	This Study
GHI42	Nahal Orvim			33.141000	35.683000	
GHI43	Nahal Orvim			33.143000	35.687000	

Continued on next page

Site	Location name	Age (ka)	$\pm 2\sigma$ (ka)	Latitude	Longitude	Age Reference
GHI44	Alonei Habashan	1436.9	19.5	33.042000	35.836000	This Study
GHI45	Alonei Habashan			33.042000	35.836000	
GHI46	Tel Saki	2744.2	47.5	32.868290	35.829050	This Study
GHI47	Dalawe	969.9	63.6	33.094000	35.752000	This Study
GHI48	Dalawe	723.1	32.4	33.085000	35.753000	This Study
GHI49	Hashirion junction	116.2	8.8	33.065000	35.749000	This Study
GHI50	Hashirion junction			33.065000	35.749000	
GHI51	Meshushim-Katzrin			33.004000	35.684000	
GHI52	Meshushim-Katzrin			33.004000	35.684000	

Table S1: Sites sampled in this study. The age for GHI02 (starred) is the average of two plateau ages in Weinstein et al. (2020), 135.5 and 123.7 ka.

Specimen	Intensity (μT)	n	FRAC	β	G_{max}	$\left\|\vec{k}\right\|$	MAD (°)	DANG (°)
GHI01B09	21.5	7	0.79	0.020	0.43	0.110	3.20	0.58
GHI02B02	23.4	8	0.89	0.030	0.35	0.090	3.44	4.09
GHI02B03	24.5	8	0.88	0.020	0.42	0.110	3.16	3.79
GHI02B07	27.7	8	0.85	0.030	0.43	0.150	3.79	4.82
GHI03A03	75.3	7	0.79	0.050	0.32	0.120	2.22	0.19
GHI03B01	69.0	7	0.80	0.020	0.37	-0.040	1.96	1.31
GHI03B03	68.2	6	0.80	0.030	0.42	-0.030	1.57	0.41
GHI03B04	74.3	9	0.82	0.040	0.49	-0.100	4.88	1.32
GHI03B05	69.1	8	0.89	0.030	0.54	0.070	1.39	0.59
GHI03B06	67.5	11	0.91	0.010	0.46	0.060	2.52	0.64
GHI03B07	68.6	10	0.90	0.030	0.48	0.000	2.12	0.74
GHI03B08	64.4	12	0.96	0.040	0.43	0.070	1.95	0.93
GHI03C01	47.6	10	0.83	0.020	0.20	-0.000	3.37	3.10
GHI03C02	51.9	10	0.80	0.020	0.22	-0.000	4.33	1.95
GHI03C04	47.5	10	0.78	0.020	0.29	-0.000	4.38	0.24
GHI03C05	42.7	11	0.84	0.010	0.22	-0.040	4.58	1.66
GHI03D01	59.1	10	0.78	0.030	0.35	-0.000	3.04	1.34
GHI03D02	58.6	9	0.83	0.030	0.35	0.150	1.29	0.50
GHI03D03	58.8	14	0.98	0.030	0.30	0.000	2.36	0.39
GHI05D03	20.8	6	0.84	0.030	0.42	0.120	4.61	1.28
GHI05E02	18.4	6	0.79	0.050	0.54	-0.000	3.80	4.67
GHI05E10	22.1	5	0.82	0.020	0.50	-0.000	3.77	1.26
GHI05E11	24.6	7	0.87	0.030	0.38	0.000	1.73	2.11
GHI05E12	27.1	5	0.78	0.030	0.52	-0.050	2.90	3.47
GHI05E13	20.9	5	0.82	0.030	0.49	-0.000	3.02	1.50
GHI05E14	27.8	6	0.85	0.040	0.45	-0.000	4.43	3.24
GHI05E15	22.9	5	0.81	0.010	0.45	-0.030	3.02	2.70
GHI06A02	25.6	7	0.78	0.020	0.45	0.070	2.57	1.40
GHI06A03	23.8	7	0.80	0.010	0.46	-0.050	1.49	0.60
GHI06A04	27.4	9	0.84	0.010	0.39	-0.040	1.20	0.61
GHI06A05	26.0	8	0.80	0.030	0.45	0.000	2.28	1.31
GHI06B02	28.4	6	0.79	0.070	0.37	0.000	1.46	0.47
GHI06B03	27.4	12	0.92	0.030	0.26	0.040	3.97	1.82
GHI06B04	27.4	11	0.93	0.020	0.31	-0.090	2.33	0.78
GHI06B05	28.5	11	0.93	0.020	0.26	0.000	3.80	0.57
GHI06C01	24.8	9	0.88	0.030	0.39	0.000	2.97	0.51
GHI06C02	27.4	10	0.85	0.020	0.36	0.010	3.18	0.65
GHI06C03	27.3	8	0.83	0.030	0.29	-0.060	3.17	0.60
GHI06C04	28.2	10	0.90	0.020	0.22	0.090	1.45	0.73
GHI06C05	25.5	8	0.80	0.020	0.27	0.060	2.09	0.71
GHI06D01	26.3	13	0.99	0.020	0.30	-0.000	3.19	0.94
GHI06D03	26.6	8	0.79	0.010	0.48	0.000	1.89	0.11

Continued on next page

Specimen	Intensity (μT)	n	FRAC	β	G_{max}	$\left\|\vec{k}\right\|$	MAD (°)	DANG (°)
GHI06D04	27.4	10	0.91	0.020	0.38	-0.010	2.46	1.44
GHI06D05	26.8	9	0.81	0.020	0.33	0.010	2.95	1.03
GHI06E01	31.4	9	0.85	0.020	0.30	0.140	1.88	1.04
GHI06E03	30.6	14	0.99	0.020	0.17	0.030	2.61	0.78
GHI06E04	28.8	14	0.99	0.020	0.21	0.150	3.69	0.96
GHI07A03	30.3	10	0.84	0.030	0.23	0.140	3.82	1.43
GHI07C02	26.4	12	0.79	0.020	0.19	-0.080	4.27	0.94
GHI07C04	23.1	15	0.81	0.010	0.17	0.070	3.00	1.07
GHI07C05	22.9	17	0.83	0.010	0.18	-0.000	2.59	1.81
GHI07C06	20.3	17	0.82	0.020	0.19	0.020	2.94	0.95
GHI07C07	23.6	11	0.83	0.020	0.18	-0.000	3.89	1.48
GHI07C08	23.8	11	0.83	0.030	0.13	-0.030	3.88	1.46
GHI07E01	37.1	5	0.80	0.060	0.50	-0.010	1.41	0.52
GHI09B01	37.5	6	0.79	0.050	0.44	-0.000	3.11	1.50
GHI09B04	29.9	11	0.81	0.030	0.38	0.070	2.93	0.81
GHI09B05	30.8	11	0.81	0.040	0.36	0.090	2.43	0.89
GHI09G01	35.0	8	0.81	0.020	0.29	0.060	4.30	5.16
GHI10B02	18.9	10	0.83	0.030	0.43	0.120	3.22	1.91
GHI18E04	33.0	11	0.79	0.010	0.30	-0.120	1.79	0.44
GHI18E05	30.0	6	0.78	0.030	0.46	-0.160	0.61	0.60
GHI18E11	37.1	6	0.80	0.030	0.40	-0.110	0.55	0.50
GHI19C03	22.3	10	0.79	0.040	0.39	0.020	4.56	3.23
GHI19C04	18.8	6	0.78	0.030	0.43	0.150	2.78	1.87
GHI19C05	25.6	7	0.84	0.050	0.37	-0.000	2.10	1.96
GHI19C06	37.0	6	0.79	0.010	0.34	-0.000	1.43	2.12
GHI19C07	19.6	9	0.80	0.040	0.47	0.060	3.78	1.36
GHI19C08	24.9	8	0.79	0.020	0.33	0.150	3.90	2.57
GHI19C09	22.3	8	0.79	0.012	0.52	0.042	4.10	1.30
GHI19C10	25.0	6	0.81	0.040	0.46	-0.050	1.20	1.36
GHI20C03	33.9	11	0.82	0.030	0.37	0.150	4.63	2.66
GHI20C04	36.5	12	0.82	0.030	0.42	0.000	3.99	3.15
GHI20C05	30.8	12	0.84	0.020	0.37	0.140	2.50	0.67
GHI20C06	33.4	12	0.82	0.030	0.35	0.070	2.41	1.18
GHI20C07	33.5	12	0.80	0.040	0.35	0.000	3.86	0.84
GHI20C08	33.6	11	0.84	0.040	0.36	-0.110	3.17	0.97
GHI20C09	33.6	12	0.83	0.030	0.38	-0.110	3.64	1.24
GHI21A04	20.1	9	0.83	0.050	0.29	-0.000	4.51	1.37
GHI21A05	22.8	8	0.79	0.020	0.33	-0.000	1.39	0.82
GHI21A06	21.5	16	0.98	0.020	0.29	-0.000	3.06	0.84
GHI21A11	25.6	15	0.88	0.020	0.25	0.060	3.85	2.57
GHI24C01	37.8	10	0.83	0.030	0.18	0.150	1.78	1.17
GHI25A04	55.4	10	0.81	0.020	0.35	0.110	2.40	1.80

Continued on next page

Specimen	Intensity (μT)	n	FRAC	β	G$_{max}$	$\left|\vec{k}\right|$	MAD (°)	DANG (°)
GHI25A08	54.7	8	0.80	0.050	0.30	0.030	2.93	2.43
GHI25A09	58.9	9	0.90	0.030	0.28	0.010	0.82	0.76
GHI25A10	63.7	11	0.81	0.020	0.20	0.020	3.85	1.97
GHI26E04	47.6	12	0.87	0.040	0.26	0.090	3.24	1.18
GHI26E08	48.9	12	0.95	0.020	0.41	0.130	1.41	0.23
GHI26E09	48.7	13	0.97	0.020	0.42	0.150	0.97	0.47
GHI26E10	47.5	9	0.84	0.020	0.60	-0.000	1.06	0.23
GHI26E13	48.9	14	0.99	0.020	0.46	0.160	1.16	0.14
GHI26E14	51.5	10	0.85	0.020	0.46	0.100	2.72	1.21
GHI27A03	37.5	11	0.85	0.020	0.32	-0.130	3.28	1.58
GHI27A05	33.9	13	0.87	0.020	0.22	-0.160	4.27	1.01
GHI27A06	40.8	12	0.79	0.030	0.33	0.000	2.35	0.83
GHI27A07	39.5	8	0.78	0.030	0.31	0.110	1.69	0.58
GHI27A08	36.6	13	0.93	0.020	0.25	0.140	4.69	1.10
GHI27A09	35.7	10	0.91	0.030	0.31	-0.000	1.24	0.98
GHI28B01	33.3	12	0.94	0.020	0.44	-0.160	0.93	0.51
GHI28B02	34.1	9	0.84	0.040	0.40	0.000	4.27	2.52
GHI28B04	34.0	11	0.91	0.010	0.41	-0.160	1.68	0.34
GHI28B06	29.0	7	0.81	0.020	0.49	-0.030	2.16	0.72
GHI28B08	31.0	10	0.80	0.020	0.57	0.000	3.18	3.87
GHI29A03	30.5	13	0.92	0.020	0.32	0.010	4.99	2.38
GHI29A04	32.8	12	0.83	0.020	0.36	0.030	4.77	1.91
GHI29A05	29.1	12	0.80	0.010	0.31	-0.090	2.52	0.73
GHI29B03	25.9	17	0.93	0.020	0.18	-0.150	2.40	1.06
GHI29B04	28.5	16	0.95	0.020	0.27	0.000	3.82	1.45
GHI29B05	29.2	15	0.93	0.010	0.27	-0.070	1.27	0.46
GHI39C02	14.9	11	0.82	0.040	0.19	0.120	4.95	4.32
GHI39C07	22.1	11	0.82	0.030	0.19	0.150	3.74	2.91
GHI39C09	16.8	12	0.92	0.030	0.23	0.000	3.22	2.73
GHI44A04	43.0	15	0.95	0.020	0.25	0.030	2.95	1.53
GHI44A05	45.2	7	0.78	0.030	0.29	0.120	1.92	2.82
GHI44A07	47.1	8	0.82	0.020	0.29	0.130	2.09	1.30
GHI44A09	45.4	12	0.94	0.030	0.28	-0.000	3.01	2.44

Table S2: Specimen that passed the specimen level CCRIT set of criteria. Intensity: paleointensity (μT), n: consecutive demagnetization steps, FRAC: fractional remanence, β = ratio of standard error to the best fit slope, G$_{max}$: maximum fractional remanence removed between consecutive temperature steps, $\vec{k}$: curvature statistic, MAD: maximum angle of deviation, DANG: deviation angle.

Site	n	Intensity (μT)	B_σ (μT)	$B_\%$ (%)	VADM (ZAm^2)	Age (Ma)	(1σ) (Ma)	Latitude (°N)	Longitude (°E)
isl013	14	41.1	2.9	7.0	57.4	0.016	0.005	64.0438	338.6420
isl011	8	27.3	2.4	8.7	38.1	0.016	0.005	64.1002	338.7528
isl007	5	15.8	2.9	18.3	22.1	0.016	0.005	64.1205	338.6838
HS92-16	8	33.0	1.4	4.3	45.7	0.016	0.005	65.4251	343.1839
kvk77	6	20.3	3.1	15.2	28.2	0.0605	0.0495	64.8167	343.5167
kvk117	7	26.0	0.9	3.6	36.2	0.0605	0.0495	64.8670	343.6500
NAL-500	4	30.3	0.8	2.8	42.2	0.0605	0.0495	64.7806	342.4887
NAL-611	14	57.6	4.6	8.0	80.1	0.0605	0.0495	64.7984	342.7997
NAL-595	7	62.4	5.3	8.6	86.8	0.0605	0.0495	64.7899	342.8177
NAL-585	6	30.9	4.3	14.0	42.9	0.0605	0.0495	65.0280	343.7710
A15	7	19.0	0.7	3.8	26.5	0.0605	0.0495	64.2018	340.9444
A24	4	62.2	5.0	8.1	86.6	0.0605	0.0495	64.6730	342.2339
A26	3	39.3	2.0	5.2	54.7	0.0605	0.0495	64.6923	342.1035
A28	4	31.2	1.9	6.0	43.6	0.0605	0.0495	63.9741	341.2078
A30	3	28.7	1.2	4.3	40.1	0.0605	0.0495	64.0614	341.4660
A31	3	59.5	0.6	1.0	83.1	0.0605	0.0495	64.1103	341.5384
A34	8	30.7	1.1	3.6	42.9	0.0605	0.0495	64.0878	340.9458
A35	4	13.1	1.0	7.4	18.3	0.0605	0.0495	64.1722	340.8615
HS92-15	8	32.1	0.4	1.2	44.5	0.0605	0.0495	65.4266	343.1844
ICE08R-14	5	28.7	0.4	1.3	40.1	0.0605	0.0495	64.2432	341.4173
ICE08R-23	3	36.1	3.8	10.4	50.4	0.0605	0.0495	64.3222	341.5395
ICE08R-24	3	35.2	3.2	9.1	49.1	0.0605	0.0495	64.3205	341.5674
A8	5	78.4	2.2	2.8	109.1	0.0605	0.0495	64.7232	340.3854
isl012	7	34.6	3.2	9.1	48.3	0.0685	0.0415	64.1155	338.8593
isl002	12	40.4	3.0	7.4	56.5	0.0685	0.0415	63.9974	338.1134
HEL-2	4	44.9	3.8	8.5	62.7	0.0685	0.0415	64.0161	338.1576
isl009	5	18.0	2.5	13.9	25.1	0.0685	0.0415	64.1154	338.7019
isl051	6	20.6	1.2	5.8	28.8	0.1555	0.1445	63.9132	342.1883
isl054	5	34.6	0.1	0.3	48.4	0.1555	0.1445	63.9174	342.2073
isl063	3	50.6	1.3	2.6	70.8	0.1555	0.1445	63.7987	341.9420
isl058	3	24.6	0.0	0.2	34.4	0.1555	0.1445	63.9178	342.2181
isl057	5	23.9	0.4	1.6	33.4	0.1555	0.1445	63.9176	342.2168
NAL-455	4	43.7	2.0	4.5	60.8	0.39	0.0	64.7384	343.3778
isl014b	5	59.0	5.3	8.9	82.5	0.59	0.19	64.0168	338.7642
NAL-460	3	25.4	1.6	6.3	35.1	0.59	0.19	65.8792	342.8444
isl020	6	30.9	0.7	2.3	43.2	2.3785	1.6215	63.9867	343.1505
isl045	3	48.3	4.4	9.1	67.5	2.47	0.12	64.0268	343.1264
NAL-365	8	35.3	1.6	4.6	49.0	2.5	2.5	65.0330	343.7670
ICE08R-15	3	33.0	1.8	5.5	45.9	2.5	2.5	64.8274	342.2445

Table S3. Pleistocene paleointensity results from Iceland (Cromwell et al., 2015b) that passed the CCRIT criteria of Cromwell et al. (2015). n: number of specimens per site, Intensity: site average intensity, Bσ: standard deviation , $B_\%$: percent error, VADM: site average VADM.

Site	n	Intensity (μT)	B$_{min}$ (μT)	B$_{max}$ (μT)	VADM (ZAm^2)	Age (Ma)	1σ (Ma)	Latitude (°N)	Longitude (°E)
A3	6	32.3	26.7	36.3	45.0	0.0605	0.0495	64.4290	339.4296
A11	7	50.4	43.6	58.4	70.2	0.0605	0.0495	64.5220	341.5283
A2	7	40.0	34.9	45.1	55.8	0.0605	0.0495	64.4488	339.4828
NAL-585	0	32.8	28.0	37.6	45.6	0.0605	0.0495	65.0280	343.7710
ICE08R-20	0	85.9	78.0	95.3	119.9	0.0605	0.0495	64.2518	341.3477
NAL-585	0	32.8	28.0	37.6	45.6	0.0605	0.0495	65.0280	343.7710
A4	7	37.7	34.5	41.1	52.5	0.0605	0.0495	64.4528	339.6939
isl009	13	16.7	14.3	18.8	23.3	0.0685	0.0415	64.1154	338.7019
isl053	11	62.6	54.7	71.5	87.5	0.1555	0.1445	63.9174	342.2106
isl014	10	75.0	66.2	84.0	104.8	0.59	0.19	64.0168	338.7642
isl018	10	44.4	37.1	52.8	62.1	0.65	2.5	63.9814	343.1202
isl042	5	49.9	45.2	57.4	69.7	1.69	2.35	64.0267	343.1223

Table S4. Pleistocene paleointensity results from Iceland (Cromwell et al., 2015b) subjected to BiCEP intensity estimation of Cych et al. (2021). n: number of specimens per site, Intensity: site average intensity, B$_{min}$, B$_{max}$: minimum and maximum intensity values from BiCEP. VADM: site VADM.

Site	n	Intensity (μT)	B_σ (μT)	$B_\%$ (%)	VADM (ZAm^2)	Age (Ma)	(1σ) (Ma)	Latitude (°N)	Longitude (°E)
mc1004	4	36.2	1.1	3.0	47.6	0.34	0.003	-77.84	166.69
mc1015	3	25.6	1.3	5.1	33.7	1.33	0.01	-77.47	169.23
mc1019	3	24.4	0.3	1.1	32.1	0.0811	0.00755	-77.88	165.30
mc1020	3	56.0	2.8	5.0	73.6	0.77	0.016	-77.88	165.02
mc1029	9	45.6	1.1	2.3	59.9	0.18	0.04	-78.31	164.80
mc1031	3	30.7	1.3	4.4	40.3	0.133	0.00585	-78.35	164.30
mc1035	3	24.8	0.6	2.4	32.6	0.12	0.01	-78.39	164.23
mc1036	3	26.0	3.3	12.6	34.1	0.12	0.02	-78.39	164.27
mc1109	3	32.5	2.3	7.1	42.7	1.261	0.02	-78.28	163.54
mc1115	5	31.3	3.6	11.5	41.1	2.46	0.155	-78.24	162.96
mc1117	4	26.6	0.2	0.7	34.9	2.28	0.12	-78.24	162.97
mc1119	4	37.5	1.8	4.8	49.3	1.08	0.11	-78.24	162.96
mc1120	3	24.1	0.3	1.1	31.7	1.756	0.025	-78.24	163.09
mc1121	6	40.4	4.7	11.7	53.1	2.505	0.03	-78.24	162.95
mc1139	3	31.2	1.3	4.1	41.0	0.882	0.04	-78.26	163.08
mc1140	3	34.7	4.6	13.4	45.6	2.043	0.045	-78.28	163.00
mc1142	4	16.0	3.9	24.4	21.0	1.225	0.01	-77.85	166.68
mc1147	3	22.7	2.7	11.8	29.8	1.63	0.16	-78.20	162.96
mc1155	3	30.0	0.2	0.6	39.5	1.5	0.025	-77.70	162.25
mc1157	4	32.8	2.4	7.3	43.2	1.71	0.005	-77.70	162.26
mc1164	3	81.8	3.3	4.1	107.7	1.364	0.05	-77.51	169.33
mc1167	3	44.4	0.1	0.3	58.4	1.38		-77.49	169.29
mc1207	3	53.2	0.5	0.9	70.0	0.5187	0.00215	-77.68	166.52
mc1217	5	30.9	4.9	16.0	40.7	0.157	0.005	-77.51	167.44
mc1218	5	34.4	2.1	6.1	45.3	0.026	0.005	-77.56	166.98
mc1306	3	6.8	0.0	0.5	9.0	2.56	0.13	-77.70	162.69

Table S5. Pleistocene paleointensity results from Antarctica (Asefaw et al., 2021) that passed the CCRIT criteria of Cromwell et al. (2015). n: number of specimens per site, Intensity: site average intensity, Bσ: standard deviation , $B_\%$: percent error, VADM: site average VADM.

Site	n	Intensity (μT)	B$_{min}$ (μT)	B$_{max}$ (μT)	VADM (ZAm^2)	Age (Ma)	1σ (Ma)	Latitude (°N)	Longitude (°E)
mc1009	5	26.2	23.3	30.1	34.5	0.074 +/- 0.0075	-77.5500	166.2000	
mc1034	6	28.2	20.6	37.3	37.0	0.3447 +/- 0.02225	-78.3900	164.2700	
mc1127	5	37.0	33.7	40.4	48.6	1.942 +/- 0.034	-78.2500	163.7300	
mc1139	7	28.8	24.7	32.4	37.8	0.882 +/- 0.04	-78.2600	163.0800	
mc1144	1	16.6	7.0	27.4	21.8	1.25 +/- 0.5	-77.8500	166.6900	
mc1147	3	21.8	18.9	25.0	28.6	1.63 +/- 0.16	-78.2000	162.9600	
mc1154	3	12.3	8.3	16.8	16.2	2.19 +/- 0.04	-77.7200	162.6300	
mc1165	5	26.8	20.7	33.3	35.3	1.451 +/- 0.03	-77.5100	169.3300	
mc1168	4	32.3	24.5	38.6	42.5	1.38 +/- 0.025	-77.4900	169.2900	
mc1200	4	22.8	19.3	26.7	30.0	0.073 +/- 0.005	-77.5500	166.1600	
mc1216	1	11.2	8.0	15.2	14.7	0.508 +/- 0.01	-77.4239	166.8108	
mc1223	2	31.7	22.8	43.5	41.7	0.378 +/- 0.014	-77.6600	166.7900	
mc1225	2	23.8	15.9	37.0	31.3	0.057 +/- 0.005	-77.5800	166.8000	
mc1303	0	10.8	6.5	14.4	14.2	0.06 +/- 0.01	-77.5800	166.2500	
mc1305	0	34.5	31.5	37.7	45.3	1.9 +/- 0.1	-78.2400	163.2300	
mc1307	0	41.0	32.5	49.8	53.9	1.33 +/- 0.12	-77.8500	166.6700	

Table S6. Pleistocene paleointensity results from Antarctica (Asefaw et al., 2021) subjected to BiCEP intensity estimation of Cych et al. (2021). n: number of specimens per site, Intensity: site average intensity, B$_{min}$, B$_{max}$: minimum and maximum intensity values from BiCEP. VADM: site VADM.

Site	n	Intensity (μT)	B_σ (μT)	$B_\%$ (%)	VADM (ZAm^2)	Age (Ma)	Latitude (°N)	Longitude (°E)
hsdp043	3	17.8	0.7	4.2	39.6	0.4451	19.76	204.95
hsdp046	3	28.5	0.9	3.1	63.6	0.4453	19.76	204.95
hsdp002	3	47.6	1.8	3.8	106.1	0.4669	19.76	204.95
hsdp041	3	46.6	2.2	4.8	103.9	0.4745	19.76	204.95
hsdp060	4	56.8	2.3	4.0	126.7	0.475	19.76	204.95
hsdp044	3	22.8	2.6	11.6	50.8	0.4915	19.76	204.95
hsdp025	3	42.8	3.4	8.0	95.5	0.4971	19.76	204.95
hsdp053	3	34.4	1.6	4.8	76.8	0.5175	19.76	204.95
hsdp051	3	30.6	0.6	1.8	68.3	0.5175	19.76	204.95
hsdp062	3	32.5	0.5	1.4	72.5	0.5203	19.76	204.95
hsdp052	3	38.3	0.2	0.5	85.5	0.53	19.76	204.95
hsdp003	3	34.9	0.0	0.0	77.9	0.5322	19.76	204.95
hsdp006	3	27.2	1.4	5.2	60.7	0.5328	19.76	204.95
hsdp056	3	35.6	0.0	0.1	79.4	0.5342	19.76	204.95
hsdp028	3	46.2	3.1	6.7	103.1	0.538	19.76	204.95
hsdp017	3	50.0	1.2	2.5	111.6	0.538	19.76	204.95
hsdp011	5	39.8	2.3	5.9	88.7	0.5381	19.76	204.95
hsdp021	4	38.5	1.3	3.3	85.9	0.5407	19.76	204.95
hsdp019	3	31.9	2.0	6.2	71.2	0.541	19.76	204.95
hsdp058	3	35.2	0.3	0.7	78.5	0.5479	19.76	204.95
hsdp034	3	34.4	0.2	0.5	76.8	0.5483	19.76	204.95
hsdp038	4	30.0	1.7	5.7	66.9	0.5484	19.76	204.95
hsdp032	4	34.6	3.1	9.0	77.2	0.5484	19.76	204.95
hsdp059	4	32.0	2.1	6.6	71.4	0.5484	19.76	204.95
hsdp024	3	31.4	2.8	8.9	70.1	0.5484	19.76	204.95
hsdp018	3	22.6	1.1	5.0	50.3	0.5498	19.76	204.95
hsdp026	3	36.4	0.2	0.4	81.2	0.5531	19.76	204.95

Table S7. Paleointensity results from Hawaii Scientific Drilling Project HSDP2 (Tauxe and Love, 2003) that passed the CCRIT criteria of Cromwell et al. (2015). n: number of specimens per site, Intensity: site average intensity, Bσ: standard deviation , $B_\%$: percent error, VADM: site average VADM.

Site	n	Intensity (μT)	B_σ (μT)	$B_\%$ (%)	VADM (ZAm^2)	Age (Ma)	Latitude (°N)	Longitude (°E)
h2a	4	59.1	2.1	3.6	131.8	0.0085	19.8278	205.0917
h2b	3	34.3	2.0	5.9	76.5	0.0085	19.8278	205.0917
h6a	6	30.5	1.3	4.3	68.0	0.03	19.8278	205.0917
h7a	4	38.3	2.8	7.2	85.4	0.0354	19.8278	205.0917
h8a	7	31.0	0.0	0.2	69.1	0.0394	19.8278	205.0917
h16a	9	26.1	1.3	5.0	58.2	0.0774	19.8278	205.0917
h20a	4	41.2	2.0	4.8	91.9	0.0875	19.8278	205.0917
h24a	3	36.4	2.7	7.5	81.2	0.10347	19.8278	205.0917
h26b	3	26.6	0.3	1.1	59.3	0.111	19.8278	205.0917
h66b	3	25.9	3.7	14.2	57.7	0.325	19.8278	205.0917
h88a	6	39.0	2.0	5.2	87.0	0.3453	19.8278	205.0917
h89a	4	31.5	2.1	6.6	70.2	0.34599	19.8278	205.0917
h98a	5	39.5	0.4	1.0	88.1	0.35425	19.8278	205.0917
h110b	3	45.7	0.0	0.1	101.9	0.3615	19.8278	205.0917
h119a	6	44.3	2.5	5.6	98.8	0.36739	19.8278	205.0917
h127a	5	29.6	0.9	3.1	66.0	0.37373	19.8278	205.0917
h136b	5	21.4	3.2	14.8	47.7	0.37962	19.8278	205.0917
h154b	6	22.5	0.7	3.1	50.2	0.39537	19.8278	205.0917
h157b	6	34.7	3.9	11.2	77.4	0.39965	19.8278	205.0917
h158a	4	30.5	1.3	4.2	68.0	0.40026	19.8278	205.0917
h161b	3	25.6	1.3	5.0	57.1	0.4027	19.8278	205.0917
h162a	3	35.3	3.9	11.1	78.7	0.40279	19.8278	205.0917
h164a	4	29.7	1.6	5.6	66.2	0.4031	19.8278	205.0917

Table S8. Paleointensity results from Hawaii Scientific Drilling Project HSDP2 (Cai et al., 2017) that passed the CCRIT criteria of Cromwell et al. (2015). n: number of specimens per site, Intensity: site average intensity, Bσ: standard deviation , $B_\%$: percent error, VADM: site average VADM.

Site	n	Intensity (μT)	B$_{min}$ (μT)	B$_{max}$ (μT)	VADM (ZAm^2)	Age Latitude (Ma)	Longitude (°N)	(°E)
h4a	17	49.7	42.6	57.4	110.8	0.016	19.8278	205.0917
h12a	10	37.8	32.6	43.5	84.3	0.0554	19.8278	205.0917
h14a	7	27.7	23.7	31.8	61.8	0.0634	19.8278	205.0917
h22b	4	14.4	10.0	18.9	32.1	0.0955	19.8278	205.0917
h59a	12	17.6	12.0	23.3	39.2	0.2981	19.8278	205.0917
h111a	8	46.5	42.4	49.5	103.7	0.3617	19.8278	205.0917
h119a	10	48.3	44.7	52.3	107.7	0.36739	19.8278	205.0917
h136b	7	16.6	12.4	20.9	37.0	0.37962	19.8278	205.0917
h168b	6	33.2	27.5	38.9	74.0	0.4	19.8278	205.0917

Table S9. Paleointensity results from Hawaii Scientific Drilling Project HSDP2 (Cai et al., 2017) subjected to BiCEP intensity estimation of Cych et al. (2021). n: number of specimens per site, Intensity: site average intensity, B$_{min}$, B$_{max}$: minimum and maximum intensity values from BiCEP. VADM: site VADM.

Site	Specimen	Intensity (μT)	n	FRAC	β	G_{max}	$\left\|\vec{k}\right\|$	MAD (°)	DANG (°)
1	1.4	3.20	8	0.82	0.056	0.3	0.068	3.6	1.3
1	1.7	4.90	8	0.81	0.048	0.32	0	3.7	1
1	1.8	3.20	5	0.81	0.044	0.5	-0.094	0.9	0.5
9	9.1	48.30	9	0.83	0.038	0.21	-0.153	1.6	0.4
9	9.2	45.50	9	0.81	0.035	0.22	-0.08	1.6	1.9
9	9.3	46.80	10	0.83	0.037	0.28	-0.119	2.9	0.5

Table S10. Paleointensity results from Galapagos (Wang et al., 2015) that passed the CCRIT set of criteria.